The EMBO Journal (2005) 24, 3266–3278 | © 2005 European Molecular Biology Organization | All Rights Reserved 0261-4189/05
www.embojournal.org

THE EMBO JOURNAL

PICK1 is a calcium-sensor for NMDA-induced AMPA receptor trafficking

Jonathan G Hanley* and Jeremy M Henley

MRC Centre for Synaptic Plasticity, Department of Anatomy, School of Medical Sciences, University of Bristol, Bristol, UK

Regulation of AMPA receptor (AMPAR) trafficking results in changes in receptor number at the postsynaptic membrane, and hence modifications in synaptic strength, which are proposed to underlie learning and memory. NMDA receptor-mediated postsynaptic Ca^{2+} influx enhances AMPAR internalisation, but the molecular mechanisms that trigger such trafficking are not well understood. We investigated whether AMPAR-associated protein–protein interactions known to regulate receptor surface expression may be directly regulated by Ca^{2+}. PICK1 binds the AMPAR GluR2 subunit and is involved in AMPAR internalisation and LTD. We show that PICK1 is a Ca^{2+}-binding protein, and that PICK1–GluR2 interactions are enhanced by the presence of 15 μM Ca^{2+}. Deletion of an N-terminal acidic domain in PICK1 reduces its ability to bind Ca^{2+}, and renders the GluR2–PICK1 interaction insensitive to Ca^{2+}. Overexpression of this Ca^{2+}-insensitive mutant occludes NMDA-induced AMPAR internalisation in hippocampal neurons. This work reveals a novel postsynaptic Ca^{2+}-binding protein that provides a direct mechanistic link between NMDAR-mediated Ca^{2+} influx and AMPAR endocytosis.

The EMBO Journal (2005) **24,** 3266–3278. doi:10.1038/sj.emboj.7600801; Published online 1 September 2005
Subject Categories: signal transduction; neuroscience
Keywords: AMPA; calcium; endocytosis; PICK1; synaptic plasticity

Introduction

Learning and memory involves changes in the molecular machinery of synapses. AMPA receptors (AMPAR) mediate the majority of fast excitatory synaptic transmission in the brain, and plasticity at excitatory synapses involves alterations in AMPAR number at the synaptic plasma membrane, brought about by regulated receptor trafficking (Carroll *et al*, 2001; Malinow and Malenka, 2002; Bredt and Nicoll, 2003). Such trafficking events require elevations in postsynaptic $[Ca^{2+}]$ (Beattie *et al*, 2000; Ehlers, 2000; Liao *et al*, 2001; Lu *et al*, 2001), but the precise molecular mechanisms for rapidly and directly transducing Ca^{2+} signals into AMPAR trafficking are not clear.

*Corresponding author: MRC Centre for Synaptic Plasticity, Department of Anatomy, School of Medical Sciences, University of Bristol, University Walk, Bristol BS8 1TD, UK. Tel.: +44 117 954 6448; Fax: +44 117 929 1687; E-mail: jon.hanley@bristol.ac.uk

Received: 11 April 2005; accepted: 9 August 2005; published online: 1 September 2005

Presynaptic trafficking of neurotransmitter-containing vesicles involves a complex array of protein–protein interactions, some of which are directly regulated by Ca^{2+}-sensing proteins (Lin and Scheller, 2000; Mochida, 2000; Augustine, 2001). Protein components differ on opposite sides of the synapse, but similarities exist in that postsynaptic AMPAR trafficking and presynaptic neurotransmitter release both involve vesicle cycling, multiple protein–protein interactions and elevations of intracellular Ca^{2+}. The Ca^{2+}-sensing protein synaptotagmin directly transduces Ca^{2+} influx into regulated protein–protein interactions to control vesicle trafficking. By analogy, it is likely that Ca^{2+}-sensitive protein–protein interactions exist postsynaptically to directly sense Ca^{2+} and control AMPAR trafficking.

AMPARs are heteromers of subunits GluR1–GluR4. GluR1/2 and GluR2/3 complexes form the majority of hippocampal AMPARs (Wenthold *et al*, 1996). Numerous proteins interact with AMPAR subunits and control trafficking to and from the postsynaptic membrane (Carroll *et al*, 2001; Barry and Ziff, 2002; Malinow and Malenka, 2002; Sheng and Kim, 2002; Bredt and Nicoll, 2003). PICK1 binds GluR2/3 and is involved in NMDA-induced internalisation of AMPAR from the plasma membrane (Xia *et al*, 2000, Iwakura *et al*, 2001, Kim *et al*, 2001; Seidenman *et al*, 2003). Little is known about the molecular mechanisms that must exist to modulate protein–protein interactions to control AMPAR trafficking.

Since PICK1 contains regions of acidic amino acids, similar to Ca^{2+}-binding sites on known Ca^{2+}-binding proteins (Ohnishi and Reithmeier, 1987; Baksh and Michalak, 1991), we considered PICK1 a likely candidate for a Ca^{2+}-sensor in AMPAR trafficking. We demonstrate that PICK1 is indeed a Ca^{2+}-binding protein. GluR2–PICK1 interactions are regulated by Ca^{2+} in a physiologically relevant range, with maximal binding at 15 μM. Overexpression in hippocampal neurons of a PICK1 mutant that binds GluR2 strongly irrespective of Ca^{2+} occludes NMDA-induced AMPAR endocytosis. This work demonstrates that the Ca^{2+}-sensing function of PICK1 is essential for the regulation of functional AMPARs available at the postsynaptic membrane.

Results

PICK1–GluR2 interaction is Ca^{2+}-sensitive

We carried out PICK1–GluR2 co-immunoprecipitations (co-IPs) from cultured hippocampal neuron extracts using anti-PICK1 antibody in a range of free $[Ca^{2+}]$ ($[Ca^{2+}]_{free}$). A robust interaction between GluR2 and PICK1 in neurons has been demonstrated before (Xia *et al*, 1999; Hanley *et al*, 2002). Figure 1A shows that GluR2 binds PICK1 weakly in low $[Ca^{2+}]_{free}$, with a ~4-fold increase in binding observed at 15 μM compared to zero $[Ca^{2+}]_{free}$. The interaction shows a biphasic Ca^{2+}-sensitivity with a significant decrease in PICK1–GluR2 binding at $[Ca^{2+}]_{free}$ higher than 15 μM. At 100 μM $[Ca^{2+}]_{free}$, the interaction is not significantly different from that at 30 μM (data not shown; Ca^{2+} buffering is

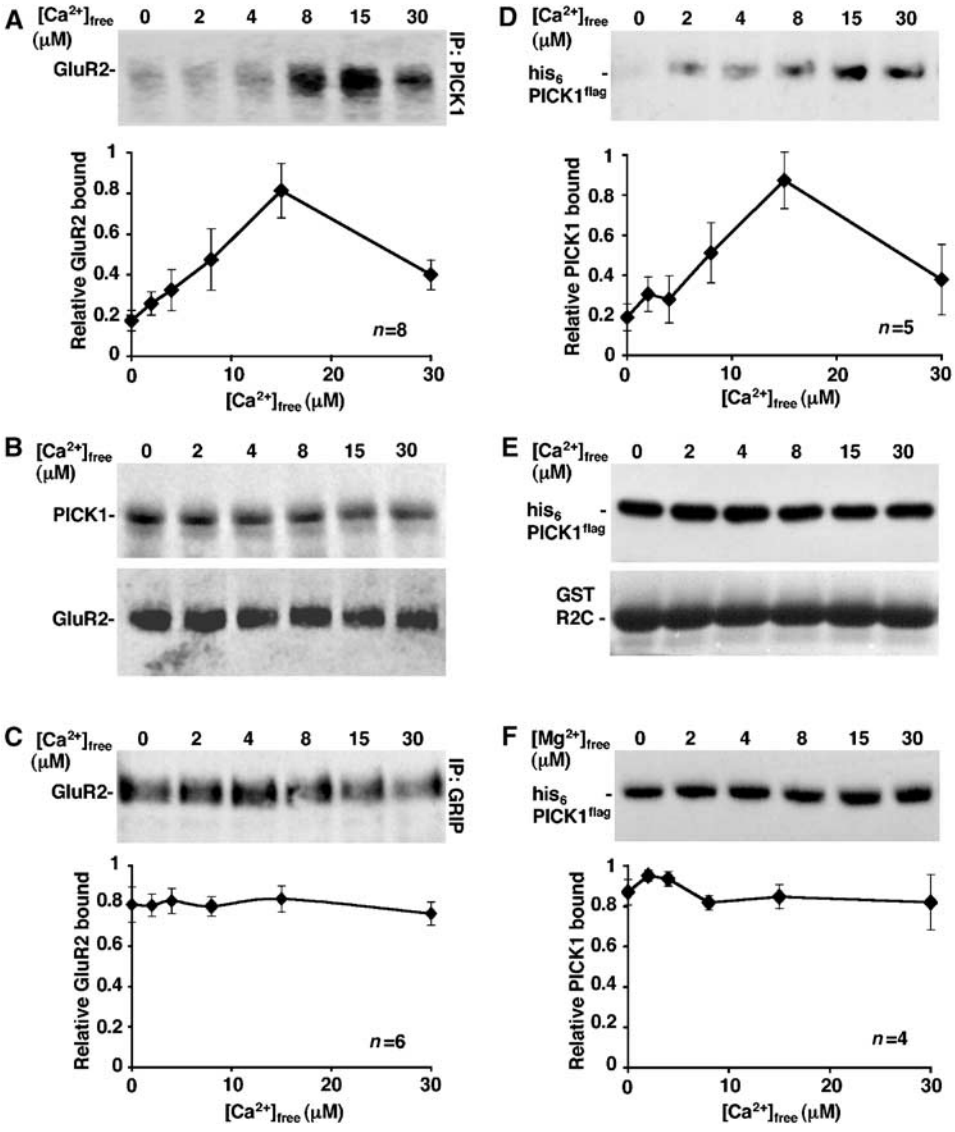

Figure 1 PICK1–GluR2 binding is Ca^{2+}-sensitive. (**A**) Endogenous PICK1–GluR2 complexes from hippocampal neurons show maximal interaction at 15 μM Ca^{2+}. Extracts of rat cultured hippocampal neurons were immunoprecipitated in different $[Ca^{2+}]_{free}$ with rabbit anti-PICK1 antibody and protein A sepharose. After washing beads in the same $[Ca^{2+}]_{free}$ buffers, bound GluR2 was analysed by Western blotting using anti-GluR2 antibody. Graph shows pooled data, $n=8$. *t*-tests 0–15 μM: $P<0.001$; 15–30 μM: $P<0.05$. (**B**) Total levels of PICK1 and GluR2 are stable in the 0–30 μM $[Ca^{2+}]_{free}$ range. (Top panel) Immunoprecipitates identical to those analysed in (A), above,were probed for PICK1 with goat anti-PICK1 antibody. (Bottom panel) Extracts of rat hippocampal neurons were prepared as above, and incubated on ice in the presence of different $[Ca^{2+}]_{free}$, in the absence of antibody. The levels of GluR2 in the extracts were analysed by Western blotting using anti-GluR2 antibody. (**C**) Endogenous GRIP–GluR2 complexes are not Ca^{2+}-sensitive. Experiments were carried out as in (A) above using anti-GRIP antibody for immunoprecipitation. Graph shows pooled data, $n=6$. (**D**) GluR2 C-terminus and PICK1 are sufficient for the Ca^{2+}-sensitive interaction. GST-R2C immobilised on glutathione beads was incubated with his_6PICK1^{flag} in the presence of different $[Ca^{2+}]_{free}$. After washing in the same $[Ca^{2+}]_{free}$ buffer, bound PICK1 was analysed by Western blotting using anti-flag antibody. Graph shows pooled data, $n=5$. *t*-tests 0–15 μM: $P<0.01$; 15–30 μM: $P<0.05$. (**E**) Total levels of his_6PICK1^{flag} and GST-R2C are stable in the 0–30 μM $[Ca^{2+}]_{free}$ range. (Top panel) His_6PICK1^{flag} was incubated in buffer A in the presence of different $[Ca^{2+}]_{free}$ as shown. The levels of PICK1 were analysed by Western blotting using anti-flag. (Bottom panel) GST-R2C immobilised on beads was treated in the same way in separate tubes and levels of GST-R2C analysed by Coomassie staining. (**F**) PICK1–GluR2 binding is not sensitive to $[Mg^{2+}]$. GST-R2C immobilised on glutathione beads was incubated with his_6PICK1^{flag} in the presence of different $[Mg^{2+}]_{free}$ as shown. After washing in the same $[Mg^{2+}]_{free}$ buffer, bound PICK1 was analysed by Western blotting using anti-flag antibody. Graph shows pooled data, $n=4$.

unreliable at this concentration). The total level of PICK1 in the IP is unaffected by changes in $[Ca^{2+}]_{free}$ in the 0–30 μM range (Figure 1B). Total GluR2 present in lysates is also unaffected by $[Ca^{2+}]_{free}$, indicating that there is no detectable Ca^{2+}-dependent proteolysis of GluR2 or PICK1 and that observed differences in GluR2 immunoreactivity are due to differential GluR2–PICK1 binding. As a control, we also carried out co-IPs using anti-GRIP antibody to test the Ca^{2+}-sensitivity of GluR2–GRIP interactions. GluR2 bound GRIP to a similar extent at all $[Ca^{2+}]_{free}$ tested (Figure 1C).

Co-IPs were carried out using neuronal extract containing a full complement of detergent-soluble neuronal proteins, some of which could play a role in the Ca^{2+}-sensitivity of the PICK1–GluR2 interaction. To investigate the molecular

requirements for this Ca^{2+}-sensitive interaction, we next analysed binding of isolated proteins. GST pull-downs using purified GST-GluR2 C-terminus (R2C) and his_6PICK1^{flag} (Hanley *et al*, 2002) demonstrate that these two proteins alone are sufficient for Ca^{2+}-sensitivity (Figure 1D). Similar to neuronal proteins, maximal binding of his_6PICK1^{flag} to GST-R2C occurs at 15 μM, with significantly weaker interactions at lower and higher $[Ca^{2+}]_{free}$. There was no detectable proteolysis of either protein at any of the $[Ca^{2+}]_{free}$ tested (Figure 1E). Importantly, binding was not affected by changes in $[Mg^{2+}]_{free}$ (Figure 1F), indicating that the interaction is specifically sensitive to Ca^{2+}. These data demonstrate that the PICK1–GluR2 interaction in neurons is sensitive to Ca^{2+}, and that PICK1 and GluR2 C-terminus mediate the Ca^{2+}-sensitivity in this interaction.

Deletion of the N-terminal acidic region in PICK1 removes the Ca^{2+}-sensitivity of the GluR2–PICK1 interaction and reduces Ca^{2+}-binding to PICK1

To analyse the role of PICK1 as a Ca^{2+}-sensor in AMPAR trafficking, we aimed to isolate a Ca^{2+}-insensitive mutant of PICK1 that could be overexpressed in cells as a dominant mutant. We focused on regions of acidic amino acids as potential regions of PICK1 that may be involved in sensing Ca^{2+}. Deletion of an N-terminal acidic region, $D^4LDYDIEED^{12}$, to make ΔNT PICK1 (Figure 2A) removes the Ca^{2+}-sensitivity of PICK1–GluR2 interaction in pull-down assays (Figure 2B). In contrast to WT PICK1, ΔNT PICK1 binds strongly to GST-R2C at all $[Ca^{2+}]_{free}$ tested. Since both WT and ΔNT PICK1 are shown on the same Western blot, absolute levels of binding for this experiment can be directly compared. There was no detectable proteolysis of his_6WT $PICK1^{flag}$, his_6ΔNT $PICK1^{flag}$ or GST-R2C at any of the $[Ca^{2+}]_{free}$ tested (Figure 2C).

Since this mutation in PICK1 affects the Ca^{2+}-sensitivity of GluR2–PICK1 binding, we tested the capacity of PICK1 to bind Ca^{2+} directly. We carried out equilibrium dialysis using $^{45}Ca^{2+}$ to analyse Ca^{2+} binding to his_6PICK1^{flag} in a range of $[Ca^{2+}]$. Figure 3A shows that WT PICK1 binds Ca^{2+}, with a B_{max} of approximately 7.5 nmol/mg PICK1 and a K_D of ~10 μM. ΔNT PICK1 binds significantly less Ca^{2+} than WT PICK1, with B_{max} ~3.5 nmol/mg and K_D ~14 μM indicating that DLDYDIEED is involved in Ca^{2+} binding. To investigate whether $D^4LDYDIEED^{12}$ is sufficient for Ca^{2+} binding, we

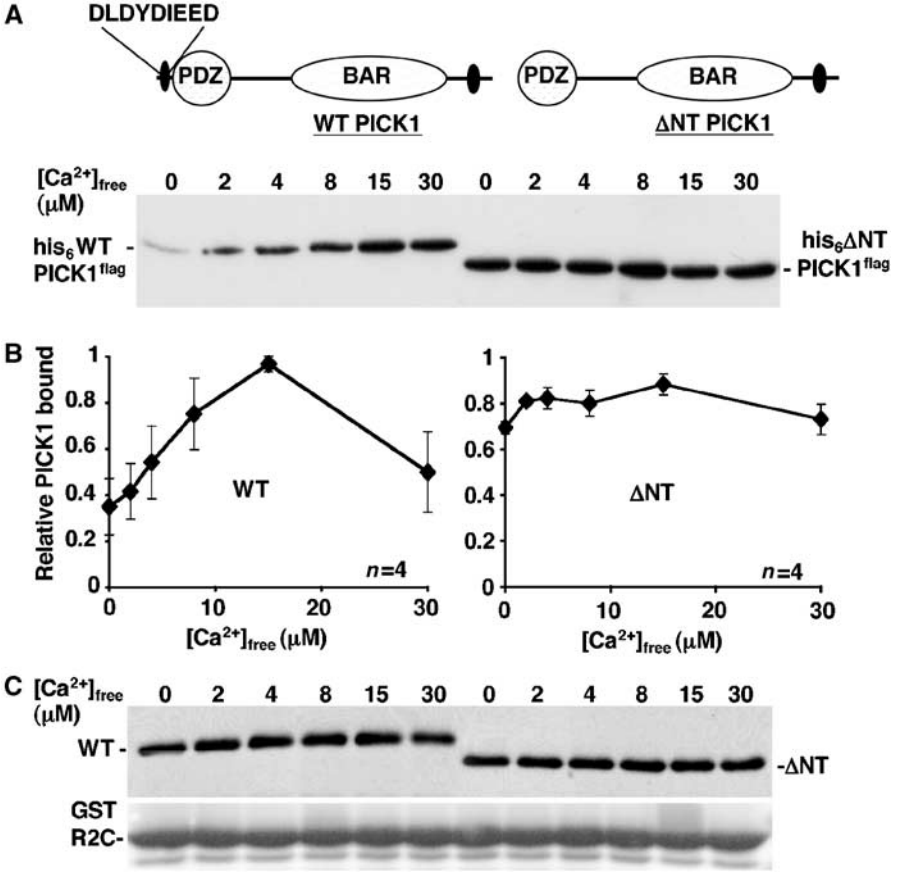

Figure 2 Deletion of the N-terminal acidic region in PICK1 removes Ca^{2+}-sensitivity of GluR2–PICK1 interaction. (**A**) WT PICK1 contains a region of acidic amino acids at the N-terminus, from residues 4–12. A mutant was constructed that lacks this region, termed ΔNT PICK1. (**B**) ΔNT PICK1 binds GluR2 C-terminus at maximal level in all $[Ca^{2+}]_{free}$ tested. GST-R2C immobilised on glutathione beads was incubated with his_6WT $PICK1^{flag}$ or his_6ΔNT $PICK1^{flag}$ in the presence of different $[Ca^{2+}]_{free}$ as shown. After washing in the same $[Ca^{2+}]_{free}$ buffer, bound PICK1 was analysed by Western blotting using anti-flag antibody. (Bottom panel) Graph shows pooled data for WT PICK1 (left) and ΔNT PICK1 (right), $n = 4$. (**C**) Total levels of his_6WT $PICK1^{flag}$, his_6ΔNT $PICK1^{flag}$ and GST-R2C are stable in the 0–30 μM $[Ca^{2+}]_{free}$ range. His_6PICK1^{flag} and his_6ΔNT $PICK1^{flag}$ were incubated in buffer A in the presence of different $[Ca^{2+}]_{free}$ as shown. GST-R2C immobilised on beads was treated in the same way in separate tubes. The levels of PICK1 were analysed by Western blotting using anti-flag and GST-R2C was analysed by Coomassie staining.

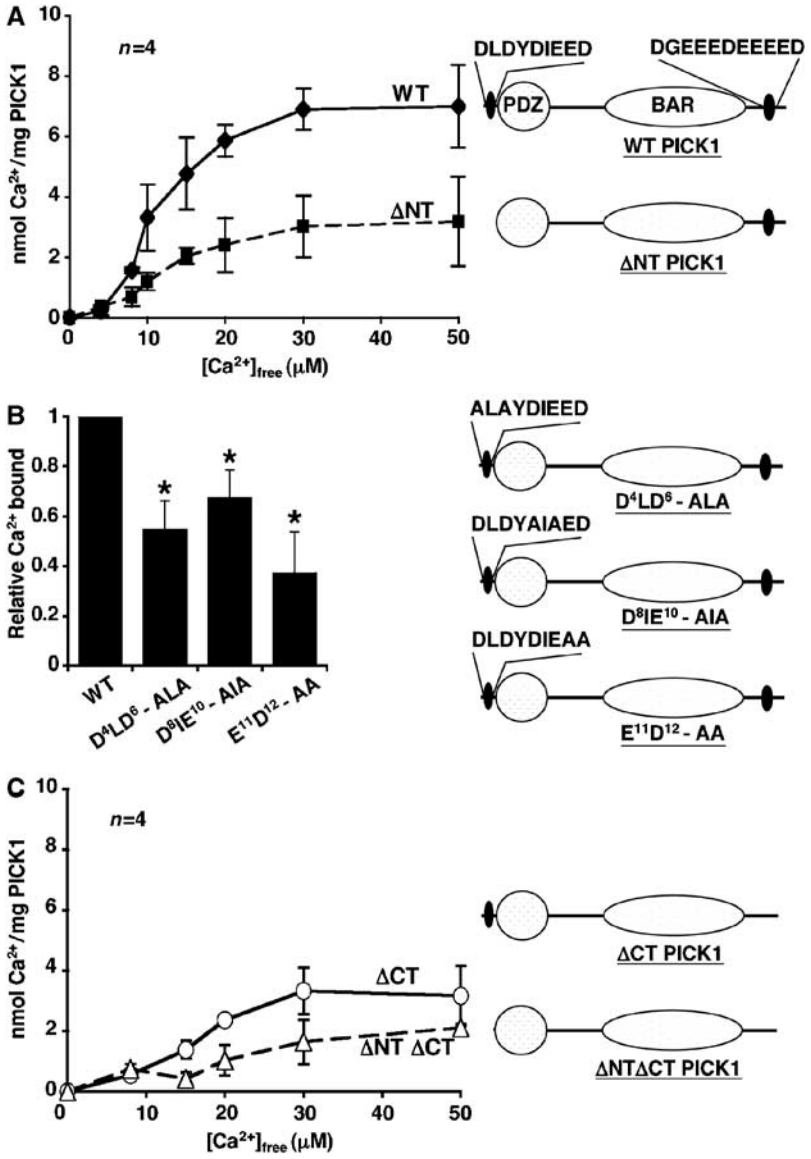

Figure 3 PICK1 is a Ca^{2+}-binding protein. (**A**) PICK1 is a Ca^{2+}-binding protein, and Ca^{2+} binding is reduced in ΔNT PICK1. Equilibrium dialysis using $^{45}Ca^{2+}$ was employed to determine the Ca^{2+} binding to known amounts of his_6WT PICK1^{flag} (solid line) and his_6ΔNT PICK1^{flag} (dashed line) in a range of $[Ca^{2+}]_{free}$ buffers. Graph shows nanomoles of Ca^{2+} bound per milligram of protein at each $[Ca^{2+}]_{free}$. Pooled data, $n=4$. Diagrams demonstrate domain mutations made in PICK1 protein. (**B**) Alanine substitutions in the N-terminal acidic region of PICK1 reduce Ca^{2+}-binding capacity. His_6PICK1 mutants as shown were subjected to equilibrium dialysis in buffer containing 15 μM $[Ca^{2+}]_{free}$. Graph shows pooled data relative to Ca^{2+}-binding values for his_6WT PICK1, $n=4$, $^*P<0.05$. Diagrams demonstrate mutations made in PICK1 protein. (**C**) A C-terminal acidic domain is also involved in Ca^{2+} binding to PICK1. His_6ΔCT PICK1^{flag} (solid line) and his_6ΔNT/ΔCT PICK1^{flag} (dashed line) were subjected to equilibrium dialysis as in (A). Graph shows nanomoles of Ca^{2+} bound per milligram of protein at each $[Ca^{2+}]_{free}$. Pooled data, $n=4$. Diagrams demonstrate domain mutations made in PICK1 protein.

fused this region to the N-terminus of a protein that does not bind Ca^{2+}. We chose β-SNAP, a protein involved in the regulation of the GluR2–PICK1 complex (Hanley *et al*, 2002). The chimeric protein DLDYDIEEDβ-SNAP did not bind significantly more Ca^{2+} than β-SNAP (data not shown), demonstrating that although DLDYDIEED is necessary, it is not sufficient for Ca^{2+} binding. To analyse in more detail the amino acids involved in Ca^{2+} binding, we mutated pairs of acidic residues in the N-terminal region to alanines and measured the Ca^{2+}-binding capacity at 15 μM Ca^{2+}. All three mutants, D^4LD^6-ALA, D^8IE^{10}-AIA and $E^{11}D^{12}$-AA showed reduced Ca^{2+} binding compared to WT PICK1 (Figure 3B), indicating that the full N-terminal acidic region is required.

The Ca^{2+} binding that remains in ΔNT PICK1 suggests the presence of a Ca^{2+}-binding site on PICK1 distinct from the N-terminal region. We therefore deleted an additional acidic region close to the C-terminus of PICK1 (D^{380}GEEEDEEEED^{390}; Figure 3C). Deletion of this region from WT PICK1 to make ΔCT PICK1 resulted in reduced Ca^{2+} binding similar to that of ΔNT PICK1. ΔCT PICK1 has a B_{max} for Ca^{2+} binding of ~3.5 nmol/mg and K_D ~16 μM. The mutant with both acidic regions deleted (ΔNTΔCT PICK1; Figure 3C) exhibits a very low level of Ca^{2+} binding, which does not saturate. These

data demonstrate that PICK1 is a Ca^{2+}-binding protein with at least two distinct domains involved in binding Ca^{2+}.

PICK1 Ca^{2+}-sensor regulates GluR2 internalisation in heterologous cells

To determine the action of Ca^{2+} on PICK1–GluR2 complexes in AMPAR trafficking, and to investigate whether the PICK1 Ca^{2+}-sensor is sufficient to control GluR2 endocytosis in a reduced system, we analysed ^{myc}GluR2 internalisation in COS cells also overexpressing PICK1^{flag} (Figure 4A). Surface-expressed ^{myc}GluR2 was labelled with anti-myc antibody on live cells, and internalised ^{myc}GluR2 visualised by acid-stripping immunocytochemistry. ^{myc}GluR2-positive structures are seen predominantly in a perinuclear location. Staining specifically represents ^{myc}GluR2 that has internalised from the plasma membrane. The ^{myc}GluR2-positive puncta localise within regions of strong PICK1 expression, but we did not observe corresponding PICK1 hot-spots, presumably because the expression level of PICK1 is sufficiently high in the surrounding cytosol to mask vesicle-associated PICK1. To elevate internal $[Ca^{2+}]$ ($[Ca^{2+}]_i$) in a graded manner, cells were exposed to different external $[Ca^{2+}]$ ($[Ca^{2+}]_O$) in the presence of the Ca^{2+} ionophore ionomycin, and then returned to medium lacking Ca^{2+}/ionomycin to allow GluR2 endocytosis to continue before processing for immunocytochemistry. We cannot define the precise $[Ca^{2+}]_i$ attained under these conditions, but it will be limited by the rate of Ca^{2+} entry via ionomycin and buffering by intracellular Ca^{2+} buffers. When WT PICK1^{flag} is expressed with ^{myc}GluR2, we observe a $[Ca^{2+}]_O$-dependent increase in internalised ^{myc}GluR2 (Figure 4A and B). Cells exposed to 2 mM $[Ca^{2+}]_O$ show a threefold enhancement in ^{myc}GluR2 endocytosis compared to those in Ca^{2+}-free conditions. Cells exposed to $[Ca^{2+}]_O$ higher than 2 mM in the presence of ionomycin are not viable. Total ^{myc}GluR2 and PICK1^{flag} expression are unaffected by exposure to ionomycin and different $[Ca^{2+}]_O$ (Figure 4C), confirming that the observed differences in internalised ^{myc}GluR2 staining are due to differential endocytosis. Cells expressing ^{myc}GluR2 in the absence of PICK1^{flag} showed basal levels of ^{myc}GluR2 internalisation at all $[Ca^{2+}]_O$ tested (Figure 4D), showing that the Ca^{2+}-sensitivity observed in Figure 4A and B is mediated by PICK1.

The GST pull-down assays show that at all $[Ca^{2+}]$ tested, ΔNT PICK1 binds GluR2 as strongly as WT PICK1 in the presence of 15 μM Ca^{2+} (Figure 2B). Therefore, ΔNT PICK1 should bind strongly to GluR2 and stimulate its endocytosis even in the absence of Ca^{2+} influx. To test this, we transfected cells with the Ca^{2+}-insensitive mutant, ΔNT PICK1^{flag} instead of WT PICK1^{flag}. In cells expressing ΔNT PICK1^{flag} and ^{myc}GluR2, a high level of ^{myc}GluR2 internalisation is indeed observed at all $[Ca^{2+}]_O$ tested, and increasing $[Ca^{2+}]_O$ has no effect on GluR2 endocytosis (Figure 4E). GluR1 subunit is present in a large proportion of endogenous AMPARs, but does not bind PICK1 (Wenthold *et al*, 1996; Xia *et al*, 1999). We therefore tested ^{myc}GluR1 in the same internalisation assay in COS cells coexpressing PICK1^{flag}. As expected, ^{myc}GluR1 shows a very low level of internalisation at all $[Ca^{2+}]_O$ tested (Figure 4F), demonstrating that the trafficking effects observed with ^{myc}GluR2 are specific for this subunit. These experiments in a reduced system strongly suggest that the Ca^{2+}-sensing role of PICK1 is sufficient to induce Ca^{2+}-dependent endocytosis of GluR2-containing AMPAR.

PICK1 is a Ca^{2+}-sensor for AMPAR trafficking in hippocampal neurons

To test the effects of the Ca^{2+}-insensitive PICK1 mutant in neurons, we made Sindbis virus encoding ΔNT PICK1^{flag}, which would act as a dominant mutant when overexpressed. Virus encoding WT PICK1^{flag} has been described previously (Terashima *et al*, 2004). The viruses are bicistronic to express EGFP in addition to PICK1. By visualisation of EGFP fluorescence, we consistently observed 80–90% neurons were infected. We carried out co-IPs in a range of $[Ca^{2+}]_{free}$ from virally infected hippocampal cultures using M2 anti-flag antibody to isolate specifically exogenous protein. WT PICK1^{flag} and ΔNT PICK1^{flag} bind endogenous GluR2/3 with a similar pattern to the GST pull-downs. As expected, ΔNT PICK1 interacts with GluR2/3 in a Ca^{2+}-insensitive manner (Figure 5B), whereas WT PICK1 binding was Ca^{2+}-sensitive, although maximal binding occurs at 8 μM $[Ca^{2+}]_{free}$ (Figure 5A). This difference may represent an influence of the GluR3 subunit, which is detected with this antibody, also binds PICK1 and is found in complex with GluR2 *in vivo* (Wenthold *et al*, 1996; Xia *et al*, 1999). As a further control, we tested GRIP1a in the same assay (Figure 5C). GRIP1a^{HA}–GluR2/3 interactions are insensitive to Ca^{2+}, exhibiting the same level of binding at all $[Ca^{2+}]_{free}$ tested.

We utilised a 'chemical LTD (chem-LTD)' protocol, whereby NMDARs are activated by bath application of NMDA to induce AMPAR internalisation in dissociated hippocampal cultures (Kameyama *et al*, 1998; Lee *et al*, 1998; Beattie *et al*, 2000; Ehlers, 2000; Colledge *et al*, 2003). We sub-

Figure 4 PICK1 Ca^{2+} sensor regulates GluR2 internalisation in heterologous cells. (**A**) COS cells coexpressing GluR2^{myc} and PICK1^{flag} exhibit Ca^{2+}-sensitive GluR2 endocytosis. COS cells cotransfected with ^{myc}GluR2 and WT PICK1^{flag} were live-labelled with rabbit anti-myc antibody. After 5 min ionomycin (1 μM) treatment in media containing different $[Ca^{2+}]_O$ as shown, cells were incubated in medium lacking Ca^{2+} for 10 min. GluR2 endocytosis was then assayed by acid-stripping immunocytochemistry. Internalised ^{myc}GluR2 was visualised with Alexa 488 and total PICK1 staining by anti-flag and Alexa 568. Representative confocal images of COS cells are shown for each condition. (**B**) Quantification of internalised ^{myc}GluR2. Values represent total internalised GluR2 (anti-myc immunoreactivity) normalised for cell area (arbitrary units). $n = 26$–28 cells per condition, $^{*}P < 0.01$; $^{**}P < 0.0001$. (**C**) Expression levels of GluR2^{myc} and PICK1^{flag} are unaffected by ionomycin and $[Ca^{2+}]_O$. Cells were treated with ionomycin and Ca^{2+} buffers as in (A), and 1% Triton X-100 extracts were analysed for total GluR2^{myc} and PICK1^{flag} expression by Western blotting using anti-myc and anti-flag antibodies, respectively. (**D**) ^{myc}GluR2 expressed in the absence of PICK1 does not exhibit Ca^{2+}-dependent increases in endocytosis. COS cells transfected with ^{myc}GluR2 alone were subjected to the same treatment as in (A). Graph shows quantification of internalised GluR2^{myc}. $n = 15$–20 cells per condition. (**E**) Ca^{2+}-insensitive ΔNT PICK1 stimulates maximal GluR2 endocytosis even in the absence of Ca^{2+} and at the same level for all $[Ca^{2+}]_O$ tested. COS cells transfected with ^{myc}GluR2 and ΔNT PICK1^{flag} were subjected to the same treatment as in (A). Graph shows quantification of internalised GluR2^{myc}. $n = 15$–20 cells per condition. (**F**) COS cells coexpressing GluR1^{myc} and PICK1^{flag} show minimal GluR1 endocytosis, which is not Ca^{2+}-dependent. Cells cotransfected with ^{myc}GluR1 and WT PICK1^{flag} were subjected to the same treatment as in (A). Graph shows quantification of internalised GluR1^{myc}. $n = 15$–20 cells per condition.

sequently monitored plasma membrane levels of GluR2-containing AMPARs by surface biotinylation. To characterise our chem-LTD, we treated untransfected cultures with NMDA and the NMDAR antagonists MK-801 and D-AP5. Treatment with 25 μM NMDA results in a significant reduction in surface GluR2, and this effect can be blocked by coapplication of 25 μM MK-801 or 50 μM D-AP5 (Figure 5D). Treatment with antagonists alone did not affect surface GluR2 levels.

Overexpression of WT PICK1 significantly enhances the NMDA-induced reduction of surface GluR2 (Figure 5E; 50% reduction, compared to 28% reduction in control cultures expressing EGFP alone). Importantly, surface AMPARs are unaffected when PICK1 is overexpressed in the absence of

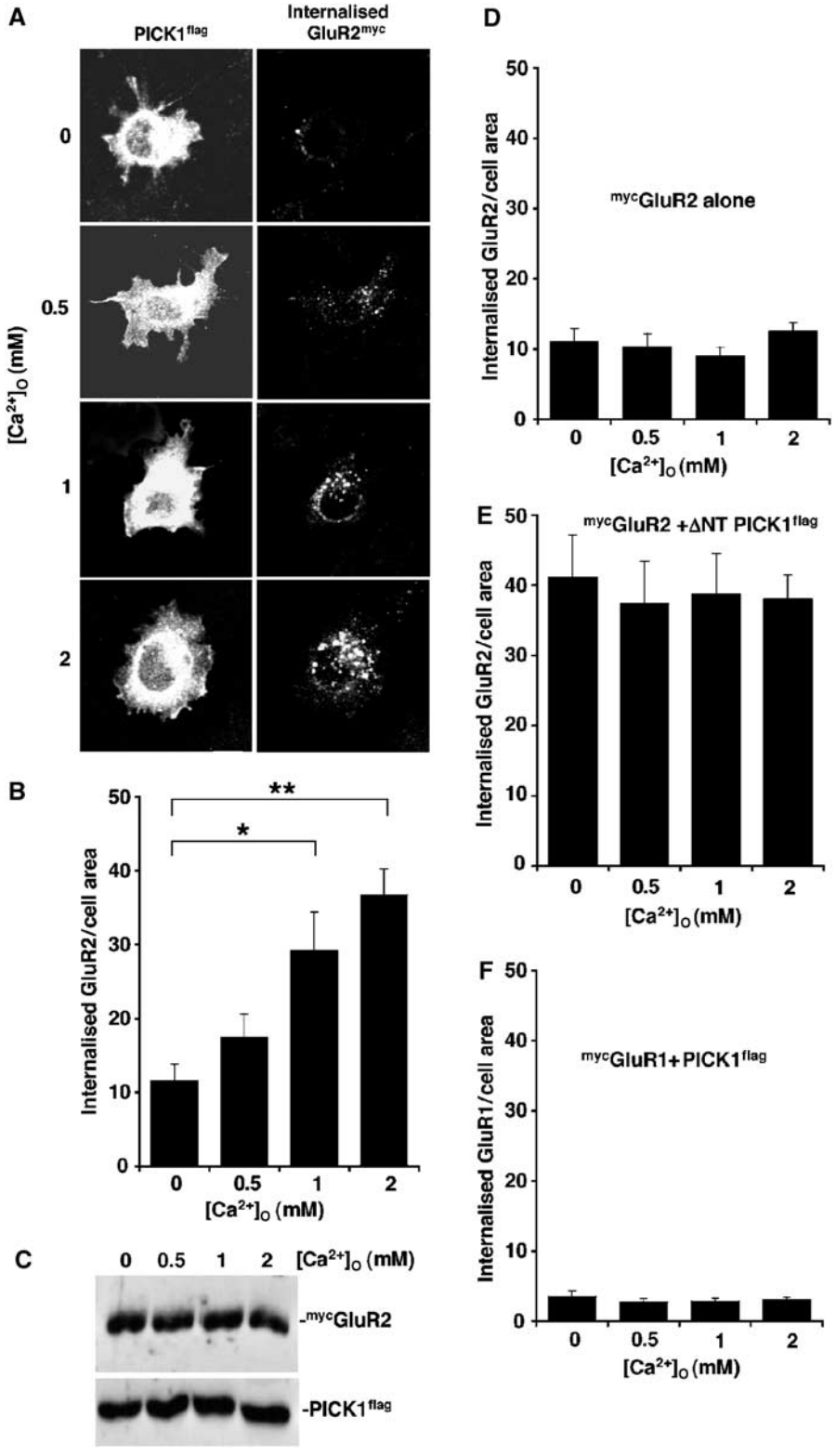

NMDA receptor activity. This demonstrates that PICK1 only stimulates AMPAR internalisation when NMDARs are activated, consistent with the requirement for a Ca^{2+} signal for optimal PICK1–GluR2 binding. Uninfected cultures (Figure 5D) and cultures infected with virus encoding EGFP alone (Figure 5E) show indistinguishable effects of NMDAR activation, indicating that viral infection *per se* has no effect on AMPAR traffic. We next tested the Ca^{2+}-insensitive mutant, ΔNT PICK1 in the same assay. Overexpression of ΔNT PICK1 reduces surface GluR2 even under conditions of NMDAR channel blockade (Figure 5F). This effect occludes chem-LTD, with no further reduction in surface GluR2 when NMDAR are activated.

To visualise the redistribution of surface GluR2 to intracellular compartments, we carried out antibody-feeding immunocytochemistry on low-density hippocampal neurons. AMPAR internalisation occurring during a short (12 min) time period is observed as subunit-immunopositive endosomes in the soma and dendrites (Beattie *et al*, 2000; Ehlers, 2000). We initially treated untransfected cultures with NMDA, MK-801 and D-AP5. Treatment with 25 μM NMDA results in a significant increase in endocytosis of GluR2-containing AMPAR, and this effect can be blocked by co-application of 25 μM MK-801 or 50 μM D-AP5 (Figure 6A). Treatment with antagonists alone does not affect AMPAR endocytosis. Uninfected cells show similar levels of NMDA-induced AMPAR endocytosis compared to controls infected with virus encoding EGFP alone (Figure 6B). A significant enhancement in NMDA-induced AMPAR internalisation is seen in cells overexpressing WT PICK1 compared to EGFP-expressing controls (Figure 6B). Consistent with the biotinylation data (Figure 5E), increased internalisation is seen specifically when NMDAR are activated. Cells overexpressing ΔNT PICK1 show an almost complete blockade of NMDA-induced AMPAR internalisation. This represents an occlusion; biotinylation experiments demonstrate that overexpression of ΔNT PICK1 results in removal of surface GluR2 even in the absence of Ca^{2+} flux through the NMDAR (Figure 5F), leaving a reduced pool for subsequent internalisation.

PICK1 binds GluR2 but not GluR1 (Xia *et al*, 1999), and it has recently been shown that PICK1 can have differential effects on GluR2 compared to GluR1 (Terashima *et al*, 2004). However, the majority of GluR1 in hippocampus is complexed with GluR2 (Wenthold *et al*, 1996). We therefore repeated chem-LTD biotinylation experiments with cultures overexpressing WT PICK1 and ΔNT PICK1 and analysed changes in surface GluR1. The same results were observed for GluR1 as GluR2, suggesting that PICK1 exerts its effects on GluR1/2 complexes (Figure 7).

Taken together, these data show that a Ca^{2+}-insensitive PICK1 mutant can over-ride a requirement for Ca^{2+} influx via NMDARs, demonstrating that the PICK1 Ca^{2+}-sensor is crucial for NMDAR-dependent internalisation of AMPAR in neurons.

Discussion

ΔNT PICK1 binds GluR2 at a high level at all [Ca^{2+}] tested, comparable to the maximal level of WT PICK1 binding at 15 μM Ca^{2+}. This suggests that in the absence of a Ca^{2+} signal, ΔNT PICK1 will bind GluR2 (in neurons or COS cells) at a level comparable to WT PICK1 at optimal [Ca^{2+}]. If PICK1 acts as a Ca^{2+}-sensor for AMPAR trafficking in living cells, the ΔNT mutant should internalise GluR2-containing receptors in the absence of a Ca^{2+} signal to a similar extent as WT PICK1 in the presence of Ca^{2+} (via NMDARs or ionomycin). We observe precisely this effect in trafficking assays in COS cells and neurons, where stimulated AMPAR endocytosis is occluded by the Ca^{2+}-insensitive mutant. In neurons expressing ΔNT PICK1, the biotinylation data demonstrate that a sizeable pool of GluR2 is redistributed away from the plasma membrane even without NMDAR activation. NMDAR activation has no further effect on surface AMPAR levels, indicating that the pool of surface AMPAR already internalised by ΔNT PICK1 is the same pool that is regulated by NMDAR activation. The acid-stripping antibody-feeding assay confirms this; NMDAR activation has no effect on AMPAR endocytosis in ΔNT PICK1-expressing cells during the experimental time period. In COS cells, where certain neuronal mechanisms may be absent, ΔNT PICK1 may enhance plasma membrane cycling of GluR2, without causing a net reduction in surface levels. Therefore, the full complement of GluR2 is available during the antibody-feeding internalisation assay. The crucial point in both experiments is that ΔNT PICK1 renders GluR2 endocytosis insensitive to the presence of a Ca^{2+} signal.

PICK1 as a Ca^{2+}-sensing molecule

We show that PICK1 directly binds Ca^{2+} in a concentration-dependent manner, the PICK1–GluR2 interaction is Ca^{2+}-

Figure 5 PICK1 is a Ca^{2+} sensor for NMDA-induced reduction in surface GluR2-containing AMPAR in hippocampal cultures. (**A**) Binding of endogenous neuronal GluR2/3 to overexpressed WT $PICK1^{flag}$ is Ca^{2+}-sensitive. Extract of rat hippocampal cultures infected with Sindbis virus encoding WT $PICK1^{flag}$-IRES-EGFP was prepared in buffer A and divided into six equal portions with a range of $[Ca^{2+}]_{free}$. Extracts were immunoprecipitated with anti-flag antibody and protein G sepharose. After washing beads in the same $[Ca^{2+}]_{free}$ buffers, bound GluR2/3 was analysed by Western blotting using anti-GluR2/3 antibody. Graph shows pooled data, $n=5$. (**B**) Binding of endogenous neuronal GluR2/3 to overexpressed ΔNT $PICK1^{flag}$ is Ca^{2+}-insensitive. As above, except that cultures were infected with virus encoding ΔNT $PICK1^{flag}$-IRES-EGFP. Graph shows pooled data, $n=5$. (**C**) Binding of endogenous GluR2/3 to overexpressed $GRIP1a^{HA}$ is not Ca^{2+}-sensitive. Extract of hippocampal cultures infected with Sindbis virus encoding $GRIP1a^{HA}$-IRES-EGFP were treated as in (A) above, except that anti-HA antibody was used for immunoprecipitation. Graph shows pooled data, $n=4$. (**D**) Characterisation of chem-LTD in uninfected cultures. Hippocampal cultures were treated with combinations of drugs as shown. In all, 50 μM APV or 25 μM MK-801 (MK) were applied for 15 min; 25 μM NMDA (N) was applied for 3 min, followed by 12 min incubation after drug washout. Biotinylation was subsequently used to quantify surface levels of GluR2. Top panel shows representative Western blot of total GluR2 present in lysates and surface (biotinylated) GluR2 after drug treatment. Graph shows pooled data presented as ratios of surface over total GluR2. $n=6$, $^{*}P<0.05$. (**E**) Overexpression of WT PICK1 in hippocampal cultures enhances NMDA-induced removal of surface GluR2, but only in the presence of NMDAR activity. Dissociated hippocampal cultures were infected with either empty-IRES-EGFP or WT PICK1-IRES-EGFP virus and exposed to 25 μM NMDA for 3 min followed by 12 min incubation after drug washout or 25 μM MK-801 for 15 min. Top panel shows representative Western blot of 25% total GluR2 present in lysates and 100% surface (biotinylated) GluR2 after treatment. Graph shows pooled data presented as ratios of surface over total GluR2. $n=7$, $^{*}P<0.05$. (**F**) Overexpression of ΔNT PICK1 in hippocampal cultures occludes NMDA-induced removal of surface GluR2. Dissociated hippocampal cultures were infected with either WT PICK1-IRES-EGFP or ΔNT PICK1-IRES-EGFP virus and exposed to drugs as above. $n=7$, $^{**}P<0.001$, $^{*}P<0.05$.

sensitive, and that mutating the N-terminal region of PICK1 reduces Ca^{2+} binding and renders the interaction with GluR2 insensitive to Ca^{2+}. Taken together, these observations indicate that PICK1 is a Ca^{2+}-sensor. Although it lacks well-characterised Ca^{2+}-binding domains such as C2 domains or EF hands, PICK1 possesses stretches of acidic amino acids, similar to those known to bind Ca^{2+} in proteins such as calreticulin and calsequestrin (Ohnishi and Reithmeier, 1987; Baksh and Michalak, 1991). These proteins also show Ca^{2+}-dependent protein–protein interactions (Michalak *et al*, 2002). The molecular mechanism for Ca^{2+} binding to acidic domains in calreticulin and calsequestrin is not well understood, but PICK1 may bind Ca^{2+} in a similar manner. Although the N-terminal acidic region, $D^4LDYDIEED^{12}$ is

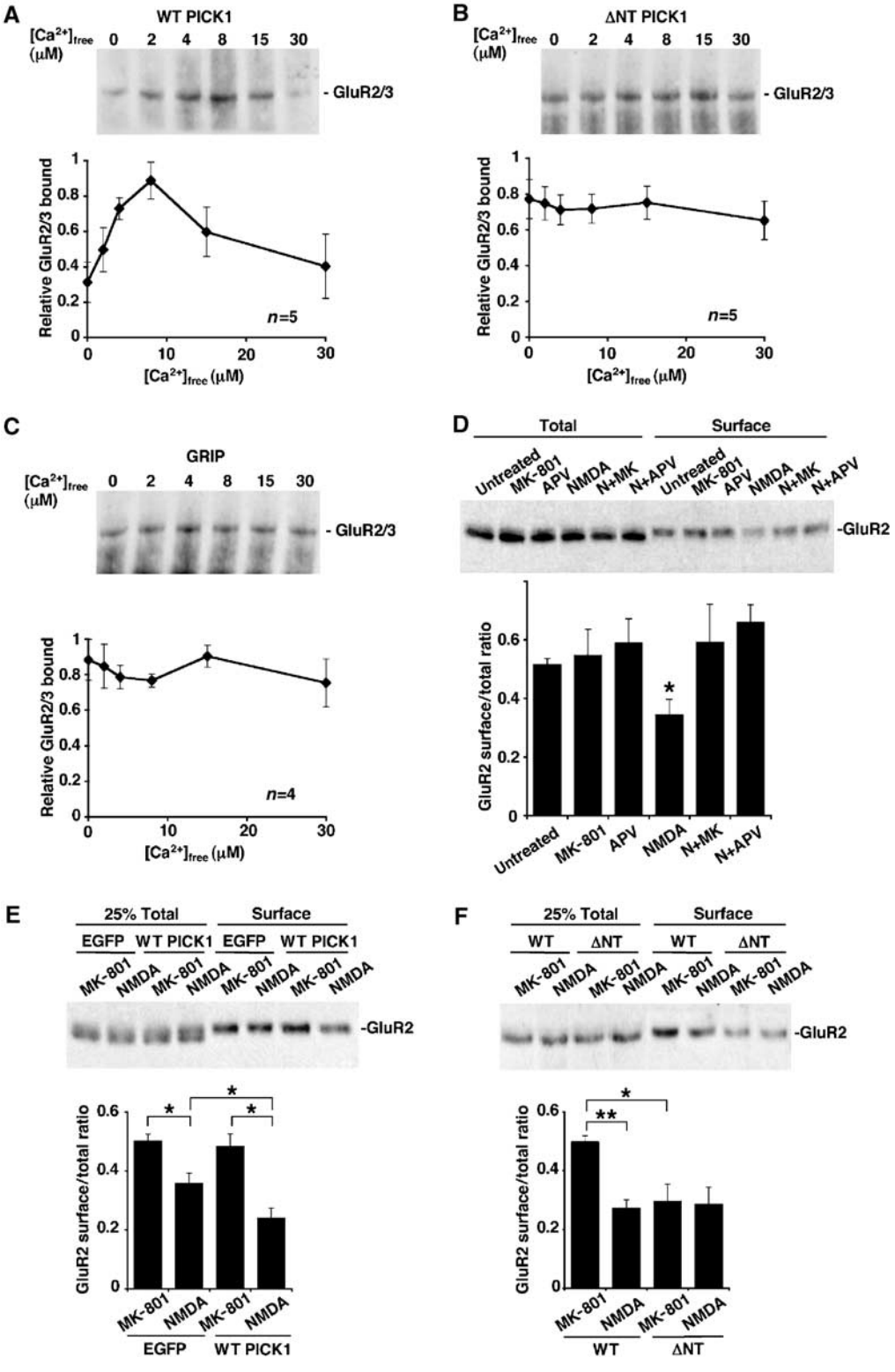

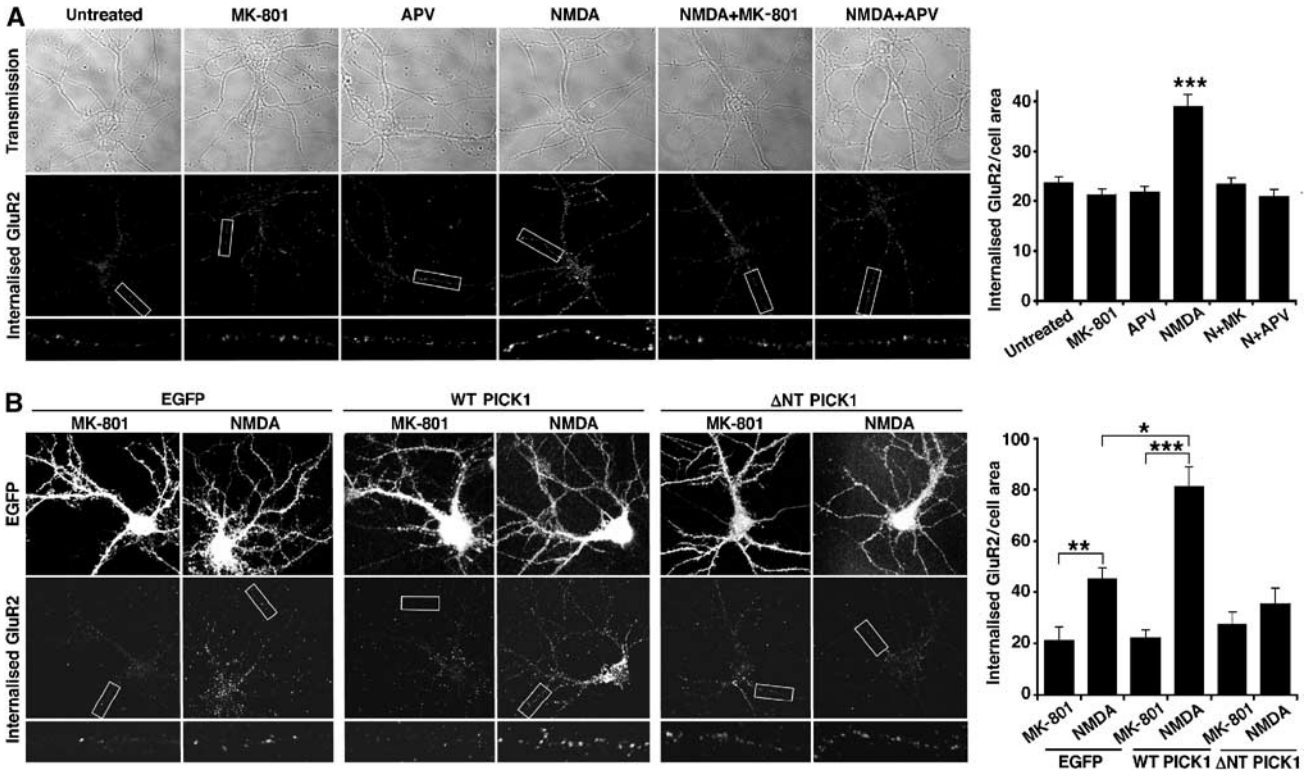

Figure 6 PICK1 is a Ca^{2+}-sensor for NMDA-induced endocytosis of GluR2-containing AMPARs in hippocampal neurons. (**A**) Characterisation of NMDA-induced GluR2 internalisation in dissociated hippocampal neurons. Low-density hippocampal cultures, live-labelled with anti-GluR2 antibody, were exposed to drugs as in Figure 5D. After acid stripping of remaining surface antibody, endocytosis of GluR2-containing AMPAR was assayed by immunocytochemistry (visualised by Alexa 568 secondary). Transmission images and internalised GluR2, including a magnified dendritic segment, are shown from representative neurons. Graph shows quantification of internalised AMPAR. Values represent total internalised GluR2 immunoreactivity normalised for cell area (arbitrary units). $n=15$ cells per condition, $***P<0.0005$. (**B**) Overexpression of WT PICK1 enhances and ΔNT PICK1 occludes NMDA-induced endocytosis of GluR2 in hippocampal neurons. Neurons were infected with virus encoding -IRES-EGFP alone, WT PICK1-IRES-EGFP or ΔNT PICK1-IRES-EGFP, live-labelled with anti-GluR2 antibody, and exposed to 25 μM NMDA for 3 min followed by 12 min incubation after drug washout or 25 μM MK-801 for 15 min. Images of EGFP fluorescence and internalised GluR2, including a magnified dendritic segment, are shown from representative neurons. Graph shows quantification of internalised AMPAR. Values represent total internalised GluR2 immunoreactivity normalised for cell area (arbitrary units). $n=15$ cells per condition, $*P<0.005$, $**P<0.001$, $***P<0.0005$.

necessary for Ca^{2+} binding to PICK1, it is not sufficient to mediate Ca^{2+} binding when fused to another protein. It is likely that the three-dimensional structure of PICK1 allows the coordination of DLDYDIEED with additional sites to mediate Ca^{2+} binding. The biphasic Ca^{2+}-sensitivity of the PICK1–GluR2 interaction suggests that Ca^{2+} may bind to multiple distinct sites on PICK1. This concept is supported by the Ca^{2+}-binding data; deletion of either the N-terminal acidic region or an acidic region close to the C-terminus (D^{380}GEEEDEEEED^{390}) significantly reduces Ca^{2+} binding, indicating that both regions are involved in binding Ca^{2+}. Unlike ΔNT PICK1, ΔCT PICK1 still binds GluR2 in a Ca^{2+}-sensitive manner (Jonathan G Hanley, unpublished observations).

PICK1 in NMDA-induced AMPAR endocytosis

At basal transmission, an equilibrium may exist between GluR2–ABP/GRIP (anchored) and GluR2–PICK1 (mobile). An important issue is how this equilibrium is altered to regulate AMPAR trafficking. Phosphorylation of GluR2 C-terminus inhibits ABP/GRIP interactions, but allows PICK1–GluR2 binding (Chung *et al*, 2000; Hayashi and Huganir, 2004). NSF disassembles GluR2–PICK1 complexes, and therefore favours AMPAR stabilisation at the plasma membrane (Hanley *et al*, 2002). Here, we demonstrate a further level of regulation capable of responding directly and immediately to a Ca^{2+} signal, in contrast to enzymatic reactions that involve multistep pathways.

Although many studies have implicated PICK1 in AMPAR internalisation and LTD (Xia *et al*, 2000; Iwakura *et al*, 2001; Kim *et al*, 2001; Perez *et al*, 2001, Hanley *et al*, 2002, Seidenman *et al*, 2003), none have determined whether it plays a permissive role (e.g. freeing AMPAR from anchoring proteins), or an active role in the process of endocytosis. COS cells do not possess membrane specialisations similar to synapses, so recombinant GluR2 is presumably not anchored at the cell surface as it would be in a neuronal environment. We show that coexpression of PICK1 with GluR2 in COS cells is sufficient to mediate Ca^{2+}-sensitive endocytosis of GluR2, whereas cells lacking exogenous PICK1 show just basal levels of GluR2 endocytosis. This suggests that PICK1 actively stimulates GluR2 internalisation. PICK1 contains a BAR domain that dimerises to form a large curved structure that either induces membrane curvature or recognises and preferentially binds to curved membranes (Peter *et al*, 2004). It is possible that on binding GluR2, PICK1 initiates the

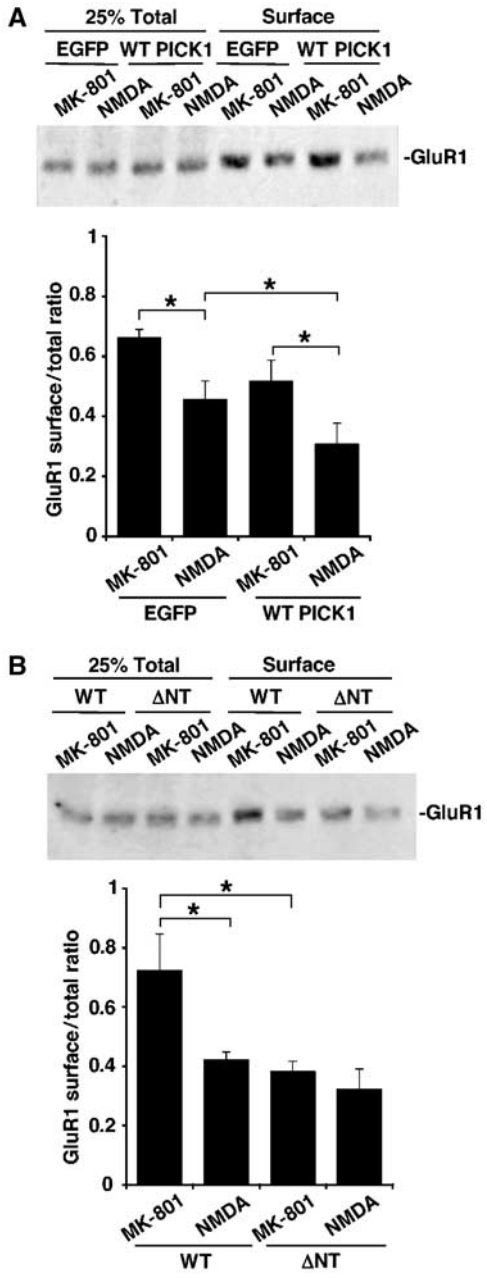

Figure 7 Ca^{2+}-sensitive PICK1 interactions influence GluR1 trafficking to the same extent as GluR2. (**A**) Overexpression of WT PICK1 in hippocampal neurons enhances NMDA-induced removal of surface GluR1. Dissociated hippocampal cultures were infected with either empty -IRES-EGFP or WT PICK1-IRES-EGFP virus and exposed to drugs as in Figure 5E. Western blots were probed with anti-GluR1 antibody. $n=5$, $^*P<0.05$. (**B**) Overexpression of ΔNT PICK1 in hippocampal neurons occludes NMDA-induced removal of surface GluR1. As above, except cultures were infected with WT PICK1-IRES-EGFP or ΔNT PICK1-IRES-EGFP virus. $n=5$, $^*P<0.05$.

formation of membrane invaginations, or alternatively, recruits GluR2 to pre-existing invaginations, most likely clathrin-coated pits, as a first step of receptor internalisation.

It has recently been shown that in the absence of NMDAR blockade, overexpressed WT PICK1 removes GluR2 subunits from the cell surface, without affecting surface GluR1 (Terashima *et al*, 2004). Here, we show that NMDAR activation is required for enhanced GluR2 internalisation by overexpressed PICK1. In the absence of NMDAR activation however, WT PICK1 overexpression does not cause GluR2 internalisation. This is consistent with the requirement for a Ca^{2+} signal (via NMDARs) for WT PICK1 to exert an effect on GluR2-containing AMPARs. In contrast to Terashima *et al* (2004), our data demonstrate that GluR1 is trafficked in a similar manner to GluR2 in WT PICK1-overexpressing cells, suggesting that the effects occur at GluR1/2 heteromers. This difference may be attributable to our bath application of NMDA that activates all surface NMDARs, as opposed to the activation of only those receptors binding synaptically released glutamate. Overexpression of the Ca^{2+}-insensitive mutant ΔNT PICK1 bypasses the requirement for NMDAR-mediated Ca^{2+} influx to trigger internalisation of both GluR1 and GluR2, resulting in a net decrease in surface AMPARs.

The low level of GluR2–PICK1 interaction at 0–4 μM Ca^{2+} does not necessarily preclude a role for this interaction in constitutive AMPAR cycling during basal transmission. It is possible that only a low level of GluR2–PICK1 binding is required for this process. However, in our experiments, WT PICK1 overexpression did not alter surface AMPARs in the absence of NMDAR activation, suggesting that this interaction is not rate limiting in constitutive AMPAR cycling.

Ca^{2+} levels in LTD

An important issue for synaptic plasticity is how can a [Ca^{2+}] increase result in either LTD or LTP? One theory for a mechanism to determine the polarity of change suggests that LTD requires a small Ca^{2+} transient, and LTP a larger one (Lisman, 1989; Artola and Singer, 1993; Cummings *et al*, 1996). We propose that the biphasic Ca^{2+} dependence of PICK1–GluR2 binding could play an important role in such mechanisms; if 15 μM Ca^{2+} is attained on LTD induction, PICK1 binding to GluR2 would mediate AMPAR endocytosis. At higher [Ca^{2+}] reached during LTP, PICK1 would not bind GluR2 efficiently, and AMPAR internalisation would be limited. Spatial and temporal qualities of Ca^{2+} transients may also be important. The source of Ca^{2+} has been shown to be crucial in determining the polarity of plasticity expressed (Nishiyama *et al*, 2000; Rose and Konnerth, 2001). A prolonged, modest rise in Ca^{2+} has been proposed to be an optimal LTD signal, in contrast to a short, high magnitude increase for LTP (Yang *et al*, 1999). It is possible that a Ca^{2+}-sensing protein will respond to specific patterns of Ca^{2+} accumulation over time, depending on the affinity and capacity of Ca^{2+} binding.

Estimates of [Ca^{2+}] attainable in dendritic spines have been extremely wide ranging: <1–40 μM have been reported (Petrozzino *et al*, 1995, Neveu and Zucker, 1996; Otani and Connor, 1998; Yang *et al*, 1999; Yuste *et al*, 1999; Franks and Sejnowski, 2002; Sabatini *et al*, 2002). Furthermore, the existence of microdomains of high [Ca^{2+}] in the immediate proximity of a Ca^{2+} channel (Llinas *et al*, 1992; Augustine, 2001) suggests that adjacent to NMDAR channels, [Ca^{2+}] will be higher than in the centre of the spine. The close proximity of NMDARs to AMPARs and therefore to potential GluR2–PICK1 interactions is likely to increase [Ca^{2+}] in the immediate vicinity of these proteins to stimulate binding. Our data indicate that ~15 μM Ca^{2+} is optimal for GluR2–PICK1 binding, suggesting that this level may be reached during LTD

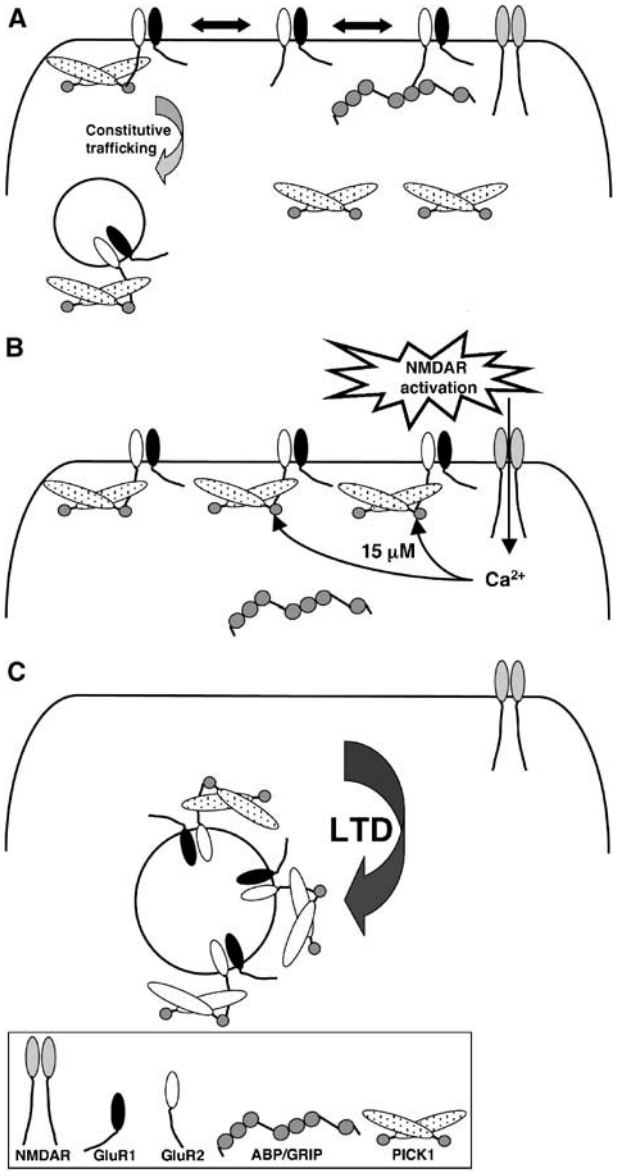

Figure 8 A model for the role of PICK1 Ca^{2+}-sensor in NMDAR-dependent AMPAR endocytosis. (**A**) Under basal conditions, when NMDARs are inactive, GluR2-containing AMPARs are either weakly bound to PICK1 or anchored by ABP/GRIP, resulting in a low level of AMPAR internalisation, representing constitutive cycling. (**B**) Activation of NMDARs localised in close proximity to AMPARs results in a Ca^{2+} flux that raises the local $[Ca^{2+}]$ to around 15 μM and therefore enhances binding of PICK1 to GluR2. (**C**) This results in increased AMPAR internalisation and hence a decrease in surface AMPAR.

induction. Figure 8 outlines a model to describe this process. The Ca^{2+} levels attained during chem-LTD have not, to our knowledge, been analysed. Homosynaptic LTD evoked by low-frequency stimulation and chem-LTD are mutually occluding, suggesting that they share the same signalling mechanisms (Lee *et al*, 1998). It is therefore predicted that the Ca^{2+} transients generated in the local spine environment during chem-LTD are similar to those in homosynaptic LTD.

The Ca^{2+}-dependent phosphatase calcineurin has previously been proposed as a primary Ca^{2+}-sensor for hippocampal LTD (Winder and Sweatt, 2001). Calcineurin dephosphorylates GluR1 resulting in reduced channel activity (Tavalin *et al*, 2002). Importantly, although GluR1 dephosphorylation has been correlated with AMPAR endocytosis (Ehlers, 2000), no causal link has been established. Here, we have described a Ca^{2+}-sensor for a protein–protein interaction crucial for AMPAR endocytosis that is directly regulated by Ca^{2+} ions, and therefore provides a mechanism for the rapid removal of surface AMPAR in direct response to a Ca^{2+} influx via NMDARs.

Materials and methods

Plasmids and purification of recombinant proteins

His_6WT and mutant $PICK1^{flag}$ were cloned by PCR and ligation into pPROExHT (GibcoBRL) or pET (Novagen). GST-R2C was described previously (Hanley *et al*, 2002). His_6PICK1^{flag} and GST-R2C were expressed in *Escherichia coli* strains DH5α or BL21. Purification of recombinant proteins was performed as described (Hanley *et al*, 2002).

Sindbis virus encoding WT $PICK1^{flag}$-IRES-EGFP was prepared as described (Terashima *et al*, 2004). ΔNT $PICK1^{flag}$-IRES-EGFP was cloned by PCR and ligation into pSinRep5 (Invitrogen). ^{myc}GluR2 unchanged at the Q/R site, and $PICK1^{flag}$ were expressed in COS cells from pcDNA3 plasmids (Perez *et al*, 2001).

Antibodies

The antibodies used were as follows: anti-GluR2 (MAB 397, Chemicon); anti-GluR2/3 (AB1506, Chemicon); anti-GluR1 (Ab-1, Oncogene); anti-PICK1 (rabbit polyclonal H-300, goat polyclonal N-18, Santa Cruz); anti-GRIP (clone 32, BD Biosciences); anti-flag (M2, Sigma); and anti-myc (A-14, Santa Cruz).

Buffers

Buffer A: 50 mM HEPES (pH 7.2), 125 mM NaCl, 1% TX-100, 5 mM HEDTA. Total $[CaCl_2]$ was added to give $[Ca^{2+}]_{free}$ according to Max Chelator software. For $[Mg^{2+}]_{free}$ buffering, 5 mM EDTA was used instead of HEDTA, with calculations determined by Max Chelator. Buffer B: 25 mM HEPES (pH 7.2), 150mM NaCl, 1% TX-100, 0.2% SDS.

GST pull-downs

GST-R2C (5 μg) was immobilised on glutathione–agarose beads. After two washes in buffer A ($+Ca^{2+}$), beads were incubated with 0.2 nM his_6WT or ΔNT $PICK1^{flag}$ in buffer A for 1 h at 4°C. After four washes with buffer A ($+Ca^{2+}$), bound protein was detected by Western blotting using anti-flag.

Neuronal cultures and Sindbis virus infections

Primary neuronal cultures were prepared from E18 Wistar rat hippocampi. For biochemical experiments, 1×10^6 cells were plated per 6 cm dish. For immunocytochemistry, 6×10^5 cells were plated per 22 mm glass coverslip. Sindbis viruses were prepared according to the Sindbis Expression System manual (Invitrogen). Infections were carried out as described (Hanley *et al*, 2002), 16–20 h before experimentation.

Co-immunoprecipitations

For co-IPs, one 6 cm dish was used per experiment (six different $[Ca^{2+}]$). Cells were lysed in 600 μl buffer A minus HEDTA plus protease inhibitor cocktail (Roche). After centrifugation, lysate was divided into 6×100 ml and 1 ml buffer A ($+Ca^{2+}$) added. Each sample was incubated at 4°C for 1 h with 2 μg H-300 anti-PICK1 antibody (Santa Cruz) or anti-GRIP antibody (BD Biosciences), followed by protein A or protein G sepharose precipitation for 1 h. Beads were washed four times with buffer A ($+Ca^{2+}$) and co-IP'ed protein detected by Western blotting. For IP of virally expressed protein, cultures infected with virus were treated as above for endogenous co-IP, except 2 μg M2 anti-flag or anti-HA was used.

Equilibrium dialysis

His_6WT $PICK1^{flag}$ and his_6ΔNT $PICK1^{flag}$ were initially dialysed overnight in buffer A lacking Ca^{2+}. Slide-a-lyzer dialysis cassettes (Pierce) containing 1 μM his_6WT PICK1 or his_6ΔNT PICK1 were incubated in 250 ml buffer A ($+Ca^{2+}$) including 0.5 MBq $^{45}Ca^{2+}$

with constant stirring for 30 h. Following incubation, three samples were taken from bath buffer and cassette and counts determined by liquid scintillation. The average counts from the bath were equated to the total Ca^{2+} concentration. Using this value, we could then determine the amount of Ca^{2+} bound to each protein by calculating the difference in radioactivity counts between bath and cassette. SigmaPlot was used to best fit a curve to give an estimate of the B_{max}, and the K_D taken as the [Ca^{2+}] at 50% of B_{max}.

Surface biotinylation and chem-LTD

After 10 min 1 μM TTX, hippocampal cultures were treated with drugs at 37°C in conditioned medium: 50 μM APV or 25 μM MK-801 for 15 min; 25 μM NMDA for 3 min, followed by 12 min incubation after drug washout at 37°C in conditioned medium. Where two drugs were applied, the same time scales were used as for single drug applications. Cultures were chilled on ice, washed in ice-cold PBS and incubated with 0.25 mg/ml Sulfo-NHS-SS-Biotin (Pierce) in PBS for 10 min on ice. After washing three times in PBS plus 1 mg/ml BSA and three times in PBS, cells were lysed in 500 μl buffer B. After centrifugation, lysate was incubated with streptavidin–agarose beads for 3 h at 4°C, washed four times in buffer B and bound protein detected by Western blotting.

Quantification of Western blots

Films of Western blots from at least four identical independent experiments were scanned and analysed using Image J. For Ca^{2+}-sensitivity of binding, the highest value was designated a score of 1, and other values taken as a proportion of this. This is used to demonstrate relative rather than absolute levels of binding in a complex. For biotinylation experiments, a ratio of values for bands representing surface over those for total GluR2 was determined for a given condition. Error bars are standard errors, and *t*-tests were carried out to determine significant differences.

Immunocytochemistry

Hippocampal neurons were surface labelled with 40 μg/ml anti-GluR2 antibody for 10 min at 37°C in conditioned medium plus 1 μM TTX and briefly washed. Cells were treated with drugs at 37°C in conditioned medium: 50 μM APV or 25 μM MK-801 for 15 min; 25 μM NMDA for 3 min, followed by 12 min incubation after drug washout at 37°C in conditioned medium. Where two drugs were applied, the same time scales were used as for single drug applications. Cells were chilled on ice, washed in ice-cold HBS and surface antibody stripped away using ice-cold 0.2 M acetic acid, 0.5 M NaCl. After four washes in ice-cold HBS, cells were fixed, permeabilised and stained with anti-mouse Alexa 568 secondary antibody (Molecular Probes).

Transfected COS cells were surface labelled with 15 μg/ml rabbit anti-myc (Santa Cruz) for 10 min at room temperature in Earle's balanced salt solution lacking Ca^{2+}/Mg^{2+} (EBSS; Gibco). They were briefly washed, then incubated in 1 μM ionomycin in EBSS plus 1 mM EGTA, 0.5, 1 or 2 mM $CaCl_2$ for 5 min at 37°C. After three washes in warm EBSS, cells were returned to 37°C for 10 min. Acid stripping was carried out as above. Cells were stained using M2 anti-flag monoclonal, and anti-mouse Alexa 568, anti-rabbit Alexa 488 secondaries.

Images were acquired on an Axiovert 200M connected to LSM510 confocal system (Zeiss). The total staining for anti-GluR2 or for anti-myc in all vesicles for a given cell was measured using Image J, and normalised for cell area. In a given experiment, data for a number of cells (*n*) were collected, error bars defined as standard errors and *t*-tests performed to determine significant differences.

Acknowledgements

We thank Tina Tang for help with COS cells, A Nishimune for Sindbis viruses, and LJ King, S Martin, J Mellor, M Ashby and G Collingridge for critical reading of the manuscript. JGH is a Wellcome Trust Career Development Fellow; the work was funded by The Wellcome Trust and the Medical Research Council.

References

Artola A, Singer W (1993) Long-term depression of excitatory synaptic transmission and its relationship to long-term potentiation. *Trends Neurosci* **16:** 480–487

Augustine GJ (2001) How does calcium trigger neurotransmitter release? *Curr Opin Neurobiol* **11:** 320–326

Baksh S, Michalak M (1991) Expression of calreticulin in *Escherichia coli* and identification of its Ca^{2+} binding domains. *J Biol Chem* **266:** 21458–21465

Barry MF, Ziff EB (2002) Receptor trafficking and the plasticity of excitatory synapses. *Curr Opin Neurobiol* **12:** 279–286

Beattie EC, Carroll RC, Yu X, Morishita W, Yasuda H, von Zastrow M, Malenka RC (2000) Regulation of AMPA receptor endocytosis by a signalling mechanism shared with LTD. *Nat Neurosci* **3:** 1291–1300

Bredt DS, Nicoll RA (2003) AMPA receptor trafficking at excitatory synapses. *Neuron* **40:** 361–379

Carroll RC, Beattie EC, von Zastrow M, Malenka RC (2001) Role of AMPA receptor endocytosis in synaptic plasticity. *Nat Rev Neurosci* **2:** 315–324

Chung HJ, Xia J, Scannevin RH, Zhang X, Huganir RL (2000) Phosphorylation of the AMPA receptor subunit GluR2 differentially regulates its interaction with PDZ domain-containing proteins. *J Neurosci* **20:** 7258–7267

Colledge M, Snyder EM, Crozier RA, Soderling JA, Jin Y, Langeberg LK, Lu H, Bear MF, Scott JD (2003) Ubiquitination regulates PSD-95 degradation and AMPA receptor surface expression. *Neuron* **40:** 595–607

Cummings JA, Mulkey RM, Nicoll RA, Malenka RC (1996) Ca^{2+} signaling requirements for long-term depression in the hippocampus. *Neuron* **16:** 825–833

Ehlers MD (2000) Reinsertion or degradation of AMPA receptors determined by activity-dependent endocytic sorting. *Neuron* **28:** 511–525

Franks KM, Sejnowski TJ (2002) Complexity of calcium signaling in synaptic spines. *Bioessays* **24:** 1130–1144

Hanley JG, Khatri L, Hanson PI, Ziff EB (2002) NSF ATPase and alpha-/beta-SNAPs disassemble the AMPA receptor–PICK1 complex. *Neuron* **34:** 53–67

Hayashi T, Huganir RL (2004) Tyrosine phosphorylation and regulation of the AMPA receptor by SRC family tyrosine kinases. *J Neurosci* **24:** 6152–6160

Iwakura Y, Nagano T, Kawamura M, Horikawa H, Ibaraki K, Takei N, Nawa H (2001) *N*-methyl-D-aspartate-induced alpha-amino-3-hydroxy-5-methyl-4-isoxazolepropionic acid (AMPA) receptor down-regulation involves interaction of the carboxyl terminus of GluR2/3 with PICK1. Ligand-binding studies using Sindbis vectors carrying AMPA receptor decoys. *J Biol Chem* **276:** 40025–40032

Kameyama K, Lee HK, Bear MF, Huganir RL (1998) Involvement of a postsynaptic protein kinase A substrate in the expression of homosynaptic long-term depression. *Neuron* **21:** 1163–1175

Kim CH, Chung HJ, Lee HK, Huganir RL (2001) Interaction of the AMPA receptor subunit GluR2/3 with PDZ domains regulates hippocampal long-term depression. *Proc Natl Acad Sci USA* **98:** 11725–11730

Lee HK, Kameyama K, Huganir RL, Bear MF (1998) NMDA induces long-term synaptic depression and dephosphorylation of the GluR1 subunit of AMPA receptors in hippocampus. *Neuron* **21:** 1151–1162

Liao D, Scannevin RH, Huganir RL (2001) Activation of silent synapses by rapid activity-dependent synaptic recruitment of AMPA receptors. *J Neurosci* **21:** 6008–6017

Lin RC, Scheller RH (2000) Mechanisms of synaptic vesicle exocytosis. *Annu Rev Cell Dev Biol* **16:** 19–49

Lisman J (1989) A mechanism for the Hebb and the anti-Hebb processes underlying learning and memory. *Proc Natl Acad Sci USA* **86:** 9574–9578

Llinas R, Sugimori M, Silver RB (1992) Microdomains of high calcium concentration in a presynaptic terminal. *Science* **256:** 677–679

Lu W, Man H, Ju W, Trimble WS, MacDonald JF, Wang YT (2001) Activation of synaptic NMDA receptors induces membrane insertion of new AMPA receptors and LTP in cultured hippocampal neurons. *Neuron* **29:** 243–254

Malinow R, Malenka RC (2002) AMPA receptor trafficking and synaptic plasticity. *Annu Rev Neurosci* **25:** 103–126

Michalak M, Robert Parker JM, Opas M (2002) Ca^{2+} signaling and calcium binding chaperones of the endoplasmic reticulum. *Cell Calcium* **32:** 269–278

Mochida S (2000) Protein-protein interactions in neurotransmitter release. *Neurosci Res* **36:** 175–182

Neveu D, Zucker RS (1996) Postsynaptic levels of $[Ca^{2+}]_i$ needed to trigger LTD and LTP. *Neuron* **16:** 619–629

Nishiyama M, Hong K, Mikoshiba K, Poo MM, Kato K (2000) Calcium stores regulate the polarity and input specificity of synaptic modification. *Nature* **408:** 584–588

Ohnishi M, Reithmeier RA (1987) Fragmentation of rabbit skeletal muscle calsequestrin: spectral and ion binding properties of the carboxyl-terminal region. *Biochemistry* **26:** 7458–7465

Otani S, Connor JA (1998) Requirement of rapid Ca^{2+} entry and synaptic activation of metabotropic glutamate receptors for the induction of long-term depression in adult rat hippocampus. *J Physiol* **511:** 761–770

Perez JL, Khatri L, Chang C, Srivastava S, Osten P, Ziff EB (2001) PICK1 targets activated protein kinase Calpha to AMPA receptor clusters in spines of hippocampal neurons and reduces surface levels of the AMPA-type glutamate receptor subunit 2. *J Neurosci* **21:** 5417–5428

Peter BJ, Kent HM, Mills IG, Vallis Y, Butler PJ, Evans PR, McMahon HT (2004) BAR domains as sensors of membrane curvature: the amphiphysin BAR structure. *Science* **303:** 495–499

Petrozzino JJ, Pozzo Miller LD, Connor JA (1995) Micromolar Ca^{2+} transients in dendritic spines of hippocampal pyramidal neurons in brain slice. *Neuron* **14:** 1223–1231

Rose CR, Konnerth A (2001) Stores not just for storage: intracellular calcium release and synaptic plasticity. *Neuron* **31:** 519–522

Sabatini BL, Oertner TG, Svoboda K (2002) The life cycle of Ca^{2+} ions in dendritic spines. *Neuron* **33:** 439–452

Seidenman KJ, Steinberg JP, Huganir R, Malinow R (2003) Glutamate receptor subunit 2 Serine 880 phosphorylation modulates synaptic transmission and mediates plasticity in CA1 pyramidal cells. *J Neurosci* **23:** 9220–9228

Sheng M, Kim MJ (2002) Postsynaptic signaling and plasticity mechanisms. *Science* **298:** 776–780

Tavalin SJ, Colledge M, Hell JW, Langeberg LK, Huganir RL, Scott JD (2002) Regulation of GluR1 by the A-kinase anchoring protein 79 (AKAP79) signaling complex shares properties with long-term depression. *J Neurosci* **22:** 3044–3051

Terashima A, Cotton L, Dev KK, Meyer G, Zaman S, Duprat F, Henley JM, Collingridge GL, Isaac JT (2004) Regulation of synaptic strength and AMPA receptor subunit composition by PICK1. *J Neurosci* **24:** 5381–5390

Wenthold RJ, Petralia RS, Blahos II J, Niedzielski AS (1996) Evidence for multiple AMPA receptor complexes in hippocampal CA1/CA2 neurons. *J Neurosci* **16:** 1982–1989

Winder DG, Sweatt JD (2001) Roles of serine/threonine phosphatases in hippocampal synaptic plasticity. *Nat Rev Neurosci* **2:** 461–474

Xia J, Chung HJ, Wihler C, Huganir RL, Linden DJ (2000) Cerebellar long-term depression requires PKC-regulated interactions between GluR2/3 and PDZ domain-containing proteins. *Neuron* **28:** 499–510

Xia J, Zhang X, Staudinger J, Huganir RL (1999) Clustering of AMPA receptors by the synaptic PDZ domain-containing protein PICK1. *Neuron* **22:** 179–187

Yang SN, Tang YG, Zucker RS (1999) Selective induction of LTP and LTD by postsynaptic $[Ca^{2+}]_i$ elevation. *J Neurophysiol* **81:** 781–787

Yuste R, Majewska A, Cash SS, Denk W (1999) Mechanisms of calcium influx into hippocampal spines: heterogeneity among spines, coincidence detection by NMDA receptors, and optical quantal analysis. *J Neurosci* **19:** 1976–1987

